DESIGN AND PROCESSING RESEARCH OF THE COMPOSITE HORN WITH CONICAL AND CYLINDER HOLE

Miaoxin XIAO* and Jun TANG

In order to meet the rapid clamping of cutting tools, it is necessary to use composite horn with conical and cylindrical hole in the vibration milling process. An equivalent model of this horn is proposed, and its frequency equation and amplification factor are established by using the equivalent four-terminal network and transfer matrix. Then, the finite element simulation analysis and vibration characteristic test of this composite horn are carried out, respectively. The results show that, compared with the design frequency, the errors of the finite calculation and the actual measurement results are 1.77% and 1.25 ‰, respectively. Through the ultrasonic milling tests on C/SiC materials, it was found that the damage pattern of the carbon fiber bundle would be suppressed.

Key words: Equivalent four-terminal network; transmission matrix; frequency equation; finite element simulation

1. Introduction

With the rapid development of aerospace, defense military, high-speed rail, wind power and precision instruments, the precision and ultra-precision machining of composite mechanical parts has attracted more and more attention. Ultrasonic assisted machining has been widely used in turning, drilling, boring, milling, and grinding because of its characteristics of reducing cutting force and prolonging tool service life [1-2].

Ultrasonic horns are the key component of the whole ultrasonic vibration system. It plays the role of amplifying amplitude and gathering energy in the vibration system, and can also match the mechanical impedance between ultrasonic load and transducer [3]. In the traditional ultrasonic assisted drilling and milling system, the connection between the ultrasonic horn and the tool head mainly includes three forms: thread cylindrical surface connection, thread positioning conical surface connection and thread conical surface end surface connection. At the same time, Dai pointed out that the horn with thread conical surface end surface connection is more conducive to the transmission of ultrasonic energy [4]. However, these three kinds of horn tool connections greatly limit the interchangeability between ultrasonic vibration system and general tools. To solve the problem of efficient and accurate tool change in ultrasonic-assisted drilling

*College of Mechanical and Electrical Engineering, Xinxiang University, Henan Xinxiang 453003, China., Email: xiaomiaoxin74@163.com

and milling system, this paper proposes to connect the tool to a horn with a conical hole and spring collet [5]. This connection method has the advantages of accurate positioning, high rotation accuracy and easy correction of tool length.

In the design process of traditional horn, the holes, chamfers and transition fillets are often ignored and simplified, inevitably leading to inaccurate design accuracy and other problems [6]. To solve the design problem of this composite horn with hole, Wang compared and analyzed the vibration characteristics of the composite horn with conical hole and cylindrical hole based on the finite element method, and concluded that the conical hole can obtain a larger amplitude ratio [7]. Ma established a frequency equation and magnification of composite ultrasonic horn with central hole based on four-terminal network method and transmission matrix method [8]. Tang studied the dynamic characteristics of the conical transition composite horn with conical hole, and analyzed the influence of the length change of each section of the composite horn on the resonant frequency, magnification and maximum stress [9]. Based on the piece-wise approximation method, Qu obtained the vibration system of exponential, conical, catenary solid and hollow half wavelength ultrasonic atomizer, and analyzed the frequency characteristics, amplitude ratio and stress distribution of the vibration system [10].

With the continuous progress of technology, multi-dimensional composite vibration horn has also been greatly developed. Li designed a Longitudinal-Bending Coupled Horn (L-BCH) of a giant magnetostrictive transducer for ultrasonic spinning process. The transducer operates at a very high frequency (18,000 to 46,000 Hz) and the tool vibrations produce about 6 amplitudes. The amplitude of the cutting tool is about 5-90 μm, which can achieve good machining quality [11]. Based on the principle of equivalent circuit, Li established a longitudinal-torsional (L&T) composite ultrasonic transducer with spiral groove. The influence of slot structure parameters on dynamic performance, such as resonant frequency, frequency interval and L&T vibration amplitude was also studied and analyzed [12]. GENG developed an ultrasonic elliptical vibration assisted reaming device and conducted experimental studies on carbon fiber reinforced material/titanium alloy laminated material [13-15]. The results show that, compared with ordinary reaming, ultrasonic elliptical vibration reaming can improve the hole quality, reduce the size error of carbon fiber reinforced material hole and titanium alloy hole, and improve tool life.

To improve the damage caused by C/SiC composite materials during traditional milling, a new ultrasonic horn that is conducive to the clamping of end milling cutters is proposed. Subsequently, the frequency equation and amplification factor of the stepped composite horn with conical hole and cylindrical hole by using four-terminal network and transmission matrix method. The frequency equation and amplification coefficient formula are used to calculate the length and amplification coefficient of each segment of the horn. It is

found that the finite element analysis results are consistent well with the experimental results. Finally, the vibration test and machining test show that ultrasonic-assisted milling of carbon/carbon fiber composite can effectively inhibit the damage form of fiber bundles.

2. Equivalent model of stepped horn with conical hole

In the ultrasonic assisted machining system, there are interfaces between the transducer and the horn and between the horn and the tool. These interfaces should be connected, and the connection mode has a great impact on the ultrasonic transmission efficiency [16]. Considering the wear of tools in rotary ultrasonic machining, it is necessary to replace in time. The spring chucks are often used to clamp the tool and connect the horn. The direct contact between the tool and the bottom of the conical hole will reduce the transmission of vibration energy at the contact interface. To this end, the conducting cylindrical hole is often set at the bottom of the conical hole. Fig. 1 shows the design of ladder horn with the cylinder hole and taper hole.

The horn is composed of conical hole and cylindrical hole. Its structure is complex and its direct design is quite cumbersome. Based on the volume equivalent transformation theory, it is equivalent to a conventional composite horn. L_1 and L_2 have a central hole of equal diameter that can be equivalent to a solid horn. L_3 can be equivalent to a cone.

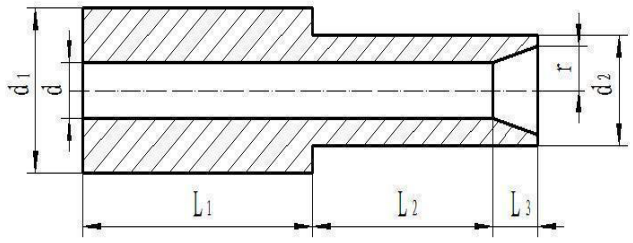

Fig. 1: Ladder horn with the cylinder hole and taper hole

The whole horn can be equivalent to a composite horn with an equal diameter rod and cone rod, as shown in Fig. 2, i.e.

$$D_1 = d_1 - d \qquad D_2 = d_2 - d \qquad D_3 = d_2 - 2r$$

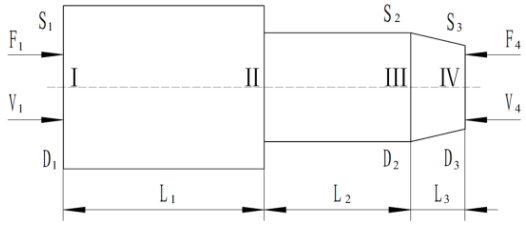

Fig. 2: Equivalent compound horn

S_1, S_2 and S_3 are the equivalent areas of the surface, and D_1, D_2 and D_3 are diameters of each section.

3. Theoretical derivation

3.1 Frequency equation

In the case of simple harmonic vibration, the wave equation of one-dimensional longitudinal vibration of variable section rod is as follows [17]:

$$\frac{\partial^2 \xi}{\partial x^2} + \frac{1}{S} \cdot \frac{\partial S}{\partial x} \cdot \frac{\partial \xi}{\partial x} + k\xi = 0 \tag{1}$$

where: $S = S(x)$ is the function of the cross-sectional area of the horn; k is the circular wave number, $k = \omega / c$; ω is the circular frequency; $c = \sqrt{E/\rho}$ is the propagation velocity of longitudinal wave in a thin rod; E is the modulus of elasticity; ρ is the density of the material, and $\xi = \xi(x)$ is the displacement function of the particle on the cross-section of the horn.

The force, vibration velocity and force impedance are respectively compared to the current, voltage and electrical admittance in the circuit by the force electric comparison method. In this way, the complex vibration system is equivalent to a simple four-terminal network, as shown in Fig. 3.

Furthermore, it can be seen that the transmission matrix of the composite horn with conical hole and cylindrical hole is shown in Eq. 2 [18-19].

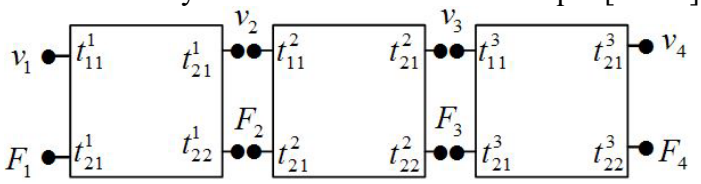

Fig. 3: The four-end network of composite horn

$$\begin{bmatrix} F_4 \\ v_4 \end{bmatrix} = \begin{bmatrix} t_{11}^1 & t_{12}^1 \\ t_{21}^1 & t_{22}^1 \end{bmatrix} \begin{bmatrix} t_{11}^2 & t_{12}^2 \\ t_{21}^2 & t_{22}^2 \end{bmatrix} \begin{bmatrix} t_{11}^3 & t_{12}^3 \\ t_{21}^3 & t_{22}^3 \end{bmatrix} \begin{bmatrix} F_1 \\ v_1 \end{bmatrix} \tag{2}$$

where: $t_{11}^1 = t_{22}^1 = \cos(kL_1)$; $t_{12}^1 = j\rho c S_1 \cos(kL_1)$; $t_{21}^1 = \frac{-j\sin(kL_1)}{\rho c S_1}$; $t_{11}^2 = t_{22}^2 = \cos(kL_2)$;

$t_{12}^2 = j\rho c S_2 \cos(kL_2)$; $t_{21}^2 = \frac{-j\sin(kL_2)}{\rho c S_2}$; $t_{22}^3 = (1-\alpha L_3)\cos kL_3 + \frac{\alpha}{k}\sin kL_3$; $t_{11}^3 = \frac{-(\alpha/k)\sin kL_3 + \cos kL_3}{1-\alpha L_3}$;

$t_{12}^3 = -\frac{j\sin kL_3}{\rho c S_2 (1-\alpha L_3)}$; $t_{21}^3 = -j\frac{\rho c S_2}{k}\left\{\left[k(1-\alpha L_3) + \frac{\alpha^2}{k}\right]\sin kL_3 - \alpha^2 L_3 \cos kL_3\right\}$.

Using the boundary condition of the horn: continuous force and displacement, the frequency equation and amplification factor of the horn can be derived. For a horn with half-wavelength or integral multiples of half wavelength,

the force on the front and rear end faces is zero (i.e. $F_1 = F_4 = 0$). Then $F_1 = F_4 = 0$ is brought into Eq.(2) to obtain:

$$\begin{bmatrix} 0 \\ v_4 \end{bmatrix} = A \begin{bmatrix} 0 \\ v_1 \end{bmatrix} = \begin{bmatrix} a_{11}^* & a_{12}^* \\ a_{21}^* & a_{22}^* \end{bmatrix} \begin{bmatrix} 0 \\ v_1 \end{bmatrix} \tag{3}$$

The frequency equation and the amplitude ratio of the two end faces can be expressed as:

$$a_{21}^* = 0 \tag{4}$$

$$M_p = \frac{v_4}{v_1} = a_{11}^* \tag{5}$$

The frequency equation of the stepped horn with conical hole can be expressed as:

$$(S_1 \tan kL_1 + S_2 \tan kL_2) \frac{-(\alpha/k)\tan kL_3 + 1}{1 - \alpha L_3} + (-S_1 \tan kL_1 \tan kL_2 + S_2) \left\{ \left[1 - \alpha L_3 + \left(\frac{\alpha}{k} \right)^2 \right] \tan kL_3 - \frac{\alpha^2 L_3}{k} \right\} = 0 \tag{6}$$

The magnification factor is

$$M_p = \left[\cos kL_1 \cos kL_2 - \frac{S_2}{S_1} \sin kL_1 \sin kL_2 \right] \frac{-(\alpha/k)\sin kL_3 + \cos kL_3}{1 - \alpha L_3}$$
$$- \left[\cos kL_1 \sin kL_2 + \frac{S_2}{S_1} \sin kL_1 \cos kL_2 \right] \left\{ \left[1 - \alpha L_3 + \left(\frac{\alpha}{k} \right)^2 \right] \sin kL_3 - \frac{\alpha^2 L_3 \cos kL_3}{k} \right\} \tag{7}$$

where $\alpha = \dfrac{D_2 - D_3}{D_2 L_3}$.

3.2 Solution calculation

To verify the feasibility of the above theoretical formula, the composite horn material designed and manufactured in this paper is 45# steel. The material property is Young's modulus of elasticity $E = 2.11 \times 10^{11} P_a$, a Poisson ratio of $\mu = 0.3$, a density of $\rho = 7852 kg/m^3$, and a longitudinal vibration sound velocity $C = 5000 \mathrm{m/s}$.

Taking a 35000Hz step horn with conical hole and central through hole as an example, since this composite horn needs to be connected with the help of a flange, the position of the flange is often set at the 1/ 4 wavelength node, and the length of the large end of the horn is set as L_1 = 40mm here. The fixed point iteration method is used to analyze the frequency equation of the composite horn, and the relationship curve between the conical hole length L_3 and the error solution of the frequency equation $\Delta L_2'$ is obtained, as shown in Fig. 4. $\Delta L_2'$ is the arithmetic difference between the result of Eq. (6) and L_2 in Table 1.

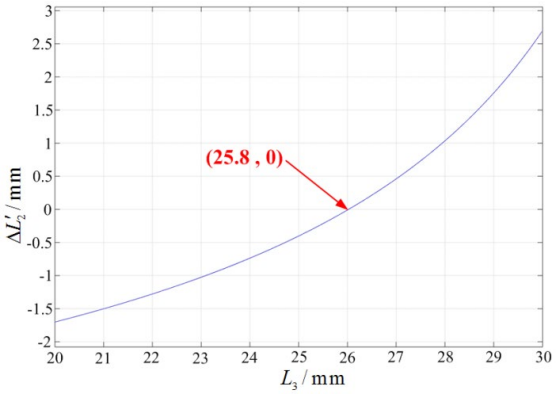

Fig. 4: The relationship between the deviation $\Delta L_2'$ and the taper hole length L_3

Through this method, three groups of composite horn are designed, as shown in Table 1.

Table 1

The size parameters of the three kinds of horns

Frequency/Hz	d/mm	d_1/mm	d_2/mm	L_1/mm	L_2/mm	L_3/mm
35000	4	30	20	40	15	25.8
28000	4	38	20	45	20	27.7
20000	4	52	20	62	38	29.6

In Table 1, d is the inner diameter.

4. Finite element verification

The vibration behavior of Langevin-type transducers based on finite element three-dimensional analysis was presented [20]. Next, the vibration characteristics of the composite horn with a flange are studied from the perspective of finite element simulation, and the proposed design theory is verified. The vibration frequency, node displacement, and amplification factor of the composite horn are compared and analyzed to verify the correctness of the theoretical formula.

4.1 Modal analysis

To meet the requirements of engineering, this horn usually needs to set a flange at the position with the minimum longitudinal amplitude (1/4 longitudinal wave wavelength). In Cimatron 3D software, based on the "bottom-up" modeling method, a 3D solid model with a flange is established according to the data of 35000Hz composite horn in Tab.1. The connecting flange with a diameter of 66mm and a thickness of 5mm is set outside. Then, the seamless connection technology is applied to transmit the 3D model to the finite element analysis

software ANSYS, and the solid95 element type is scanned to generate the volume grid type. The natural mode of the composite horn is extracted by block lanczo method. Fig. 5 is the longitudinal vibration displacement distribution diagram of 35000Hz horn with a flange.

It can be seen from Fig. 5 that the natural frequency of the composite ultrasonic vibration horn is 34710Hz; the amplitude magnification is 2.83, and the minimum ultrasonic amplitude is located at the connecting flange.

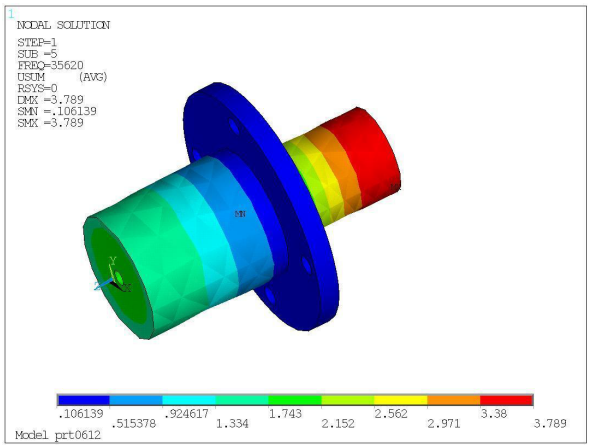

Fig. 5: Longitudinal vibration displacement distribution of 35000Hz horn

The same method is used for the finite element analysis of 28000Hz and 20000Hz in Tab.1, and the results are shown in Tab. 2. It can be seen from Tab. 2 that, comparing the theoretical calculation with the finite element analysis, the resonant frequency of finite element analysis is basically consistent with the design frequency, and the relative error rate is 1.27-1.77%. The amplification factor calculated by the derived amplification factor formula is slightly smaller than the finite element analysis value, and the relative error rate is 1.9-8.8%. Through comprehensive analysis, the derived frequency equation and amplification factor formula can meet the engineering application design requirements of horn with the conical hole and central through hole.

Table 2

Calculation and simulation results of natural mode of composite horn

Design frequency (f/Hz)	Finite element value (f'/Hz)	Amplification factor (Mp)	Finite element value (Mp')	Frequency error (%)	Amplitude error (%)
35000	35620	2.6	2.83	1.77	8.8
28000	28457	3.51	3.79	1.63	7.98
20000	20253	6.82	6.95	1.27	1.9

The main reasons for finite element errors include: (1) the flange of the composite horn changes its original stiffness/mass ratio, resulting in a deviation of

its natural frequency; (2) compared with one-dimensional wave theory, the finite element method can comprehensively take into account the mutual influence of longitudinal and transverse waves on the frequency of composite horns; (3) there is a deviation between the theoretical characteristic parameters of the finite element input material and the actual engineering characteristic parameters.

4.2 Harmonic response analysis

Taking the 35000Hz horn with a flange as an example, the mode superposition method is selected to analyze the harmonic response of the model; the time history analysis method is applied to measure the output side 211# nodes of the model to obtain the harmonic response analysis curve. The results are shown in Fig. 6. It can be seen that the resonant frequency of the horn is 34710Hz.

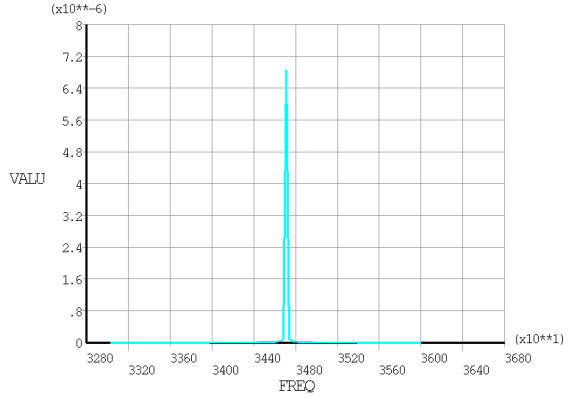

Fig. 6: The Harmonic response curve of 35000Hz ultrasonic horn

5. Test verification

5.1 Vibration effect test

Based on the above related design theory, the 35000Hz stepped composite horn with conical hole and cylindrical hole is fabricated and connected with a standard half wavelength 35000Hz transducer. The impedance analyzer developed by Beijing Confederation times is used for performance test, and the results are shown in Fig. 7.

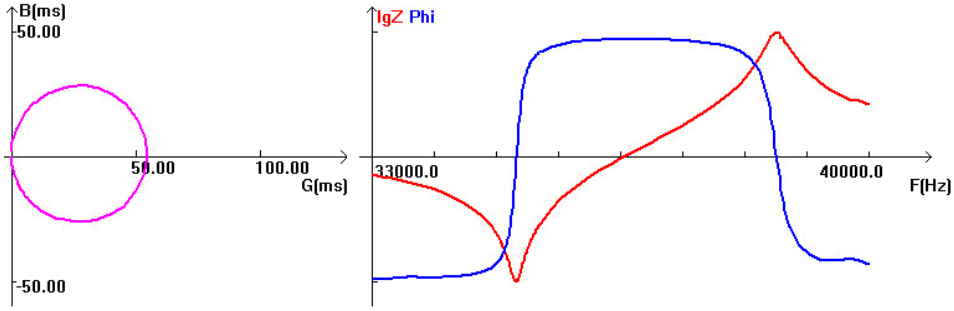

(a) Admittance circle diagram (b) Frequency impedance diagram

Fig. 7: Impedance measurement results

It can be seen from Fig. 7(a), the curve formed by the conductivity G and admittance B of the transducer is circular and regular. From the curves in Fig.7 (b) showing the relationship between frequency F, impedance lgZ and phase Phi, it can be seen that the mechanical vibration frequency of the stepped composite horn with conical hole and cylindrical hole is 35044hz.The error rate relative to the design frequency of 35000Hz is 1.25 ‰, which is mainly caused by the processing and manufacturing accuracy of each part and instrument measurement error. It meets the application requirements of self-developed 35000 ± 500Hz ultrasonic power supply.

Lk-g10 series laser displacement sensor provided by Keith company of Japan is selected to measure the vibration amplitude of the composite horn, as shown in Fig. 8.

According to the test results in Fig. 8, the ultrasonic amplitude is stable and reliable. The ultrasonic amplitude is 7.35μm.

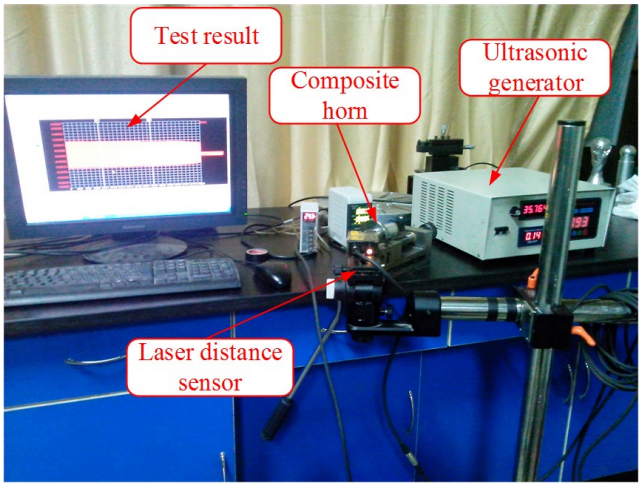

Fig. 8: The ultrasonic amplitude test site

5.2 Processing effect test

On VMC8150 machining center, the milling experiments of carbon/silicon carbide materials processed by ordinary machining and ultrasonic machining are compared and analyzed. The switching between the two processing modes is realized by turning on/off the ultrasonic power supply. Among them, the spindle speed of NC machining center is $N = 1200r/\min$; the feed rate of each tooth $f_z = 0.02mm$, and the milling depth $a_p = 0.15mm$.

After processed, JSM6390LV scanning electron microscope produced by Japan Electronics Co., Ltd. is used to test the two processed specimens, and the test results are shown in Fig. 9.

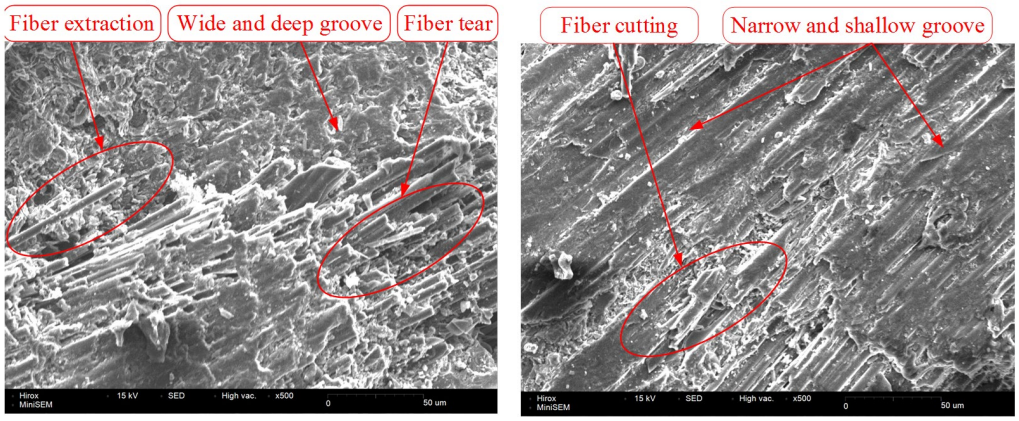

(a) Common milling surface (b) Ultrasonic milling surface

Fig. 9 The SEM images of milling C/SiC workpiece surface morphology

It can be seen from Fig. 9 that under ordinary milling conditions, wide and deep grooves appear on the surface of the specimen, and defects such as pulling out and tearing of carbon fiber bundles appear on the surface; Under the condition of ultrasonic milling, the surface of the specimen is relatively flat; the surface groove is relatively narrow and shallow, and the carbon fiber bundle is mainly cut.

6. Conclusions

Based on the principle of equivalent volume transformation, the equivalent model of stepped composite horn with conical hole and central through hole is established. Based on the equivalent four-terminal network and transmission matrix method in the one-dimensional vibration principle, the frequency equation and amplification coefficient equation of the equivalent composite step horn are obtained. The mechanical structure parameters of each section are achieved by using the fixed point iteration method. The modal analysis and harmonic response

analysis of the developed ultrasonic vibration system verify the correctness of the theoretical calculation and analysis of the system. The results show that the resonant frequency of the vibration system is 35044Hz and the ultrasonic amplitude is 6.5μm. Compared with traditional processing methods, ultrasonic vibration can effectively suppress the pull-out and tear of carbon fiber bundles.

In the future, the thermodynamic characteristics of the work-piece surface and the change law of tool wear state after ultrasonic vibration is applied to the tool would be studied.

Author Contributions

Miaoxin Xiao proposed the research derived the theoretical formulas; Jun Tang conducted finite element correlation analysis on the ultrasonic horn; Miaoxin Xiao and Jun Tang wrote the manuscript. The authors have read and approved the manuscript.

REFERENCES

[1] *Luo, X., Chen, Y., Li, W., Lv, B., & Zhang, P.,* Design and optimization of stepped compound horn based on finite element method. Journal of Physics: Conference Series, vol.2037, no.1, pp. 012003, 2021. DOI: 10.1088/1742-6596/2037/1/012003

[2] *Asmael, M., Safaei, B., Zeeshan, Q., Zargar, O., & Nuhu, A. A.,* Ultrasonic machining of carbon fiber–reinforced plastic composites: a review. The International Journal of Advanced Manufacturing Technology, vol.113, pp.3079-1320, 2021. https://doi.org/10.1007/s00170-021-06722-2

[3] *Tang, Y., & Lin, S.,* Analysis on electric impedance-controlled active ultrasonic horn in radial vibration. Ultrasonics, vol. 131, pp. 106938, 2023. https://doi.org/10.1016/j.ultras.2023.106938

[4] *Dai, X.G., Gu, Z.W., Fu, S.G., Zhang, X.Z.,* Relation between amplified pole link structure and energy transmission. Journal of Tsinghua University (Science and Technology), vol.44, no.2, pp.160-162, 2004. DOI: 10.16511/j.cnki.qhdxxb.2004.02.005

[5] *Lin, S.Y., Wang, S.J., Fu, Z.Q., Hu, J., Wang, C.H., Mo, R.Y.,* Radial vibration for a radially polarized piezoelectric composite transducer. Acta Acustica, vol.38, no.3, pp.354-363, 2013. DOI: 10.15949/j.cnki.0371-0025.2013.03.011

[6] *Banerjee, B., Pradhan, S., Das, S., Chakraborty, A., & Dhupal, D.,* Horn design and analysis in ultrasonic machining process using ANSYS. Advances in Materials and Processing Technologies, vol.8, no. sup3, pp.1359-1372, 2022. https://doi.org/10.1080/2374068X.2021.1945266

[7] *Wang, W.G., He, X.P.,* Study on the different shapes of ultrasonic horn with a central hole. Journal of Shaanxi Normal University(Natural Science Edition), vol.43, no.4, pp.43-47, 2015. DOI: 10.15983/j.cnki.jsnu.2015.04.244

[8] *Ma, F.J., Kang, R.K., Dong, Z.G., Liu, Y., Sha, Z.H., Zhang, S.F.,* Design and analysis on compound ultrasonic horn with center hole. Journal of Machine Design, vol.32, no.6, pp.51-55, 2015. DOI: 10.13841/j.cnki.jxsj.2015.06.011

[9] *Tang, J., Zhao, B.,* Design and dynamic analysis on the composite horn with taper hole. Journal of Applied Acoustics, vol.36, no.3, pp.234-240, 2017. DOI: 10.11684/j.issn.1000-310X.2017.03.007

[10] *Zhai, D.G., Xiang, D., Mo, P., Wang, H., Liu, N., Duan, G.H.,* Design of ultrasonic atomizer vibration system based on piecewise approximation method. Journal of Mechanical Engineering, vol.48, no.21, pp.47-56, 2012. DOI: 10.3901/JME.2012.21.047

[11] *Li, P., Chen, Y., Li, W., Sun, J., Li, J., & Wang, K.,* Design of Longitudinal-Bending Coupled Horn of a Giant Magnetostriction Transducer. Actuators, vol.11, no.4, pp.110, 2022. https://doi.org/10.3390/act11040110

[12] *Li, H., Chen, T., Song, H., Wang, Q., & Ye, J.,* Design and experimental study of longitudinal-torsional ultrasonic transducer with helical slots considering the stiffness variation. The International Journal of Advanced Manufacturing Technology, vol.114, pp.3093-3107, 2021. https://doi.org/10.1007/s00170-021-06802-3

[13] *Geng, D., Zhang, D., Li, Z., & Liu, D.,* Feasibility study of ultrasonic elliptical vibration-assisted reaming of carbon fiber reinforced plastics/titanium alloy stacks. Ultrasonics, vol.75, pp.80-90, 2017. https://doi.org/10.1016/j.ultras.2016.11.011

[14] *Geng, D., Teng, Y., Liu, Y., Shao, Z., Jiang, X., & Zhang, D.,* Experimental study on drilling load and hole quality during rotary ultrasonic helical machining of small-diameter CFRP holes. Journal of Materials Processing Technology, vol.270, pp.195-205, 2019. https://doi.org/10.1016/j.jmatprotec.2019.03.001

[15] *Geng, D., Lu, Z., Yao, G., Liu, J., Li, Z., & Zhang, D.,* Cutting temperature and resulting influence on machining performance in rotary ultrasonic elliptical machining of thick CFRP. International Journal of Machine Tools & Manufacture, vol.123, pp.160-170, 2017. https://doi.org/10.1016/j.ijmachtools.2017.08.008

[16] *Ryndzionek, R., & Sienkiewicz, Ł.,* A review of recent advances in the single-and multi-degree-of-freedom ultrasonic piezoelectric motors. Ultrasonics, vol.116, pp.106471, 2021. https://doi.org/10.1016/j.ultras.2021.106471

[17] *Afshari, M., & Arezoo, B.,* A new design of wide blade ultrasonic horns using Non-Uniform Rational B-Spline shaped slots. Applied Acoustics, vol.196, pp. 108871, 2022. https://doi.org/10.1016/j.apacoust.2022.108871

[18] *Ouyang, J., Qiu, Z., & Zhang, Y.,* Design and development of two-dimensional ultrasonic horn with B-spline curve based on orthogonal method. Ultrasonics, vol.123, pp.106713, 2022. https://doi.org/10.1016/j.ultras.2022.106713

[19] *Yang, J. J., Fang, Z. D., Wei, B. Y., & Deng, X. Z.,* Theoretical explanation of the 'local resonance' in stepped acoustic horn based on Four-End Network method. Journal of Materials Processing Technology, vol.209, no.6, pp.3106-3110, 2009. https://doi.org/10.1016/j.jmatprotec.2008.07.018

[20] *Iula, A., Vazquez, F., Pappalardo, M., & Gallego, J. A.,* Finite element three-dimensional analysis of the vibrational behaviour of the Langevin-type transducer. Ultrasonics, vol.40, no.1-8, pp. 513-517, 2002. https://doi.org/10.1016/S0041-624X(02)00174-9